Investigation of Corrosion Fatigue Phenomena in Transient Zone of Mechanical Drive Steam Turbines and its Preventive Measures

by

Satoshi Hata
Engineering and Design Division
Mitsubishi Heavy Industries, Compressor Corporation

Naoyuki Nagai
Hiroshima Research & Development Center
Mitsubishi Heavy Industries, Ltd.

Norihito Fujimura
MCO Saudi Arabia, LCC. (MCOSA)
Mitsubishi Heavy Industries, Compressor Corporation

Satoshi Hata

Satoshi Hata is a Group Manager within the Turbo Machinery Engineering Department, Mitsubishi Heavy Industries, Ltd., in Hiroshima, Japan. He has 30 year experience in R&D for nuclear uranium centrifuges, turbomolecular pumps, heavy-duty gas turbines, steam turbines and compressors. Mr. Hata has B.S., M.S. and Ph.D. degrees (in Mechanical Engineering) from Kyusyu Institute of Technology.

Naoyuki Nagai

Naoyuki Nagai is a Research Manager in the Research & Development Center, at Mitsubishi Heavy Industries, Ltd., in Hiroshima Japan. He has 27 year experience in R&D and troubleshooting for rotor dynamics, torsional dynamics involved in electromagnetic, control and aerodynamic coupling regarding about compressor, steam turbine and driving system. Mr. Nagai received his B.S. and M.S. degrees from Kyushu Institute of Technology and Ph.D. from Hiroshima University (in Mech. Engineering).

Norihito Fujimura

Norihito Fujimura is an application engineer of Engineering Department in Global Marketing & Sales Division, Mitsubishi Heavy Industries, Compressor Corporation, in Tokyo, Japan. He has eight years' experience in designing compressors and steam turbines. Mr. Fujimura has B.S and M.S degrees in Mechanical Engineering from Oita University

ABSTRACT

For mechanical drive steam turbines, the investigation results of corrosion fatigue phenomena in the transient zone are introduced, including basic phenomena on expansion line and actual design and damage experience. These results were analyzed from the standpoint of stress intensity during the start of cracking. In order to resolve such problems, preventive coating and blade design methods against fouling and corrosive environments are developed. Detailed evaluation test results are given for coating performance using a unique test procedure simulating fouling phenomena and washing conditions. Finally, the results of the successful modification of internals and on-line washing results on site are introduced.

INTRODUCTION

In petrochemical plants, the flow path of process gas compressor drive steam turbines have several kinds of potential damage [1] such as erosion and corrosion, resulting in deterioration of performance and a decrease in strength margin. Especially, in the process of steam expansion, depending on steam pressure and temperature, corrosive chemicals in very low levels of concentration tend to be enriched to a high level. These enriched chemicals deposit on the internal parts of the steam turbine and cause a decrease in strength or blade failure [2].

In this paper, the authors investigate the relationship between this enrichment zone, strength safety margin, and blade failure, and the root causes according to analysis of actual blade failures. Based on these investigation results, the authors introduce blade structure improvements in order to increase the safety margin for corrosion fatigue.

As one of the factors related to performance deterioration and operation restriction, fouling on nozzle and blade profiles has to be highlighted, and it is necessary to think of some improvements for the prevention of fouling. The authors study surface treatment methods applicable to

actual blades to improve anti-corrosion and anti-fouling. They also introduce a new surface treatment method and the results of an evaluation test for coating functions, including washing efficiency using a unique simulation test set-up. Finally, the possibility of long-term effective operation based on a combination of a new surface treatment method, new online washing system and special flow path design is explained.

Turbine Expansion Line and Typical Damage
In the physical process of the low pressure stages of a steam turbine expanding from the superheated zone to the saturated zone, possible causes of mechanical damage are shown in Figure 1. On dry and wet areas around the saturation line, we tend to observe SCC caused by high concentrated NaOH, pitting, corrosion fatigue related to NaCl enrichment in the special zone (Wilson zone) in which dry and wet conditions continuously occur in the moisture range of 2% to 6% and heavy drain erosion in high moisture zones of over 12%.   As shown in Figure 2, a fatigue endurance limit for 13Cr stainless steel under NaCl distilled water decreases drastically, and in this Wilson zone we have to pay particular attention to blade design, whilst considering the critical importance of controlling impurities in steam for actual continuous operation. It is necessary to understand the corrosive environment in actual operation to evaluate fatigue life. However, it is very difficult to expect concentration level changes of corrosive chemicals under conditions of rapid expansion in complicated high velocity flow fields. In this sense, it is important to evaluate mechanical integrity with a combination of detailed static and dynamic stress analysis and operation experience.
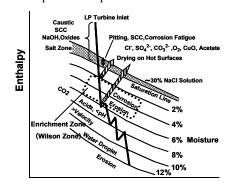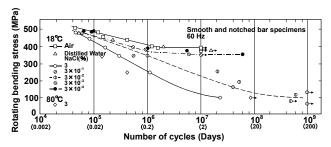

Figure 1. Turbine Expansion Line and Typical Damage [3]

Figure 2.   Decrease of Fatigue Endurance Limit for 13Cr Stainless Steel under NaCl Distilled Water [4]

Case Study of Typical Low Pressure Blade Damage and Root Cause Analysis
Figure 3 shows a typical failure of blades in the low pressure section (tenon and finitely grouped type of L-1 stage) [5]. The tenon and shroud plate have failed. Detailed conditions of the fracture surface and crack propagation direction (arrows) are shown in Figure 4. This is conformed cracking initiated on the internal side of the tenon and this failure is HCF according to the observed fine spacing striation [6].

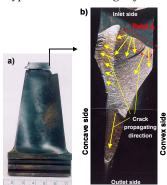*Figure 3 Typical Blade Damage of LP Section*

Figure 4 Crack Propagation on Fracture Surface

Detailed fracture and stress analyses of the actual blade are carried out by root cause analysis, which is shown in Figure 5. Key factors involved in this failure could include excessive static and dynamic external forces, and a decrease in the fatigue endurance limit in a corrosive environment. It is also important to evaluate resonance stress in the variable speed range in such a corrosive environment.
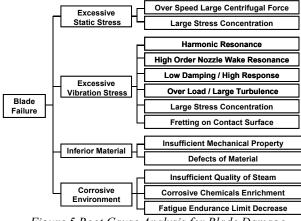

Figure 5 Root Cause Analysis for Blade Damage

Enrichment of Corrosive Chemicals in Steam and Corrosion Fatigue

In order to investigate the relationship between corrosion fatigue and the wet/dry transient zone, a detailed analysis of the fracture surface and corrosion chemicals deposited on an actual damaged rotor is carried out.

As a result of the fracture surface analysis shown in Figure 6, the typical corrosion pits of diameter about 20 micrometers in diameter are observed around the fatigue crack starting point. Though corrosion fatigue includes environmental factors, it is difficult to quantitatively estimate the actual operating condition affecting the fatigue limit, and there are a lot of other unclear factors. A basic mechanism of corrosion fatigue is explained in Figure 7 [9] [16] . This corrosion fatigue phenomenon is affected by certain types of chemical materials and their concentration levels, and it is thought that concentration cell effect and selective passive film formation cause material embitterment.
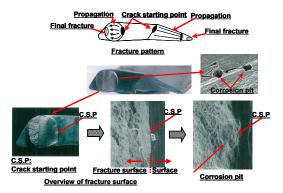

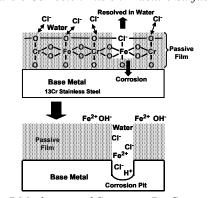*Figure 6 Corrosion Pits on Fracture Surface*

Figure 7 Mechanism of Corrosion Pit Generation

Considering the fact that several typical corrosion pits are observed, it is easy to expect a very severe corrosive environment under high concentration of corrosive chemicals. In order to define this severe corrosive environment, a concentration analysis of deposits on the fracture surface is carried out. As indicated in Figure 8, the concentration of Na and Cl are at a maximum of 4000 ppm and that of K is 1700ppm; these levels are relatively high.
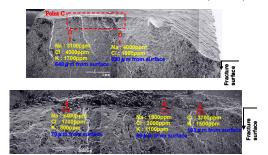

Figure 8 Corrosive Chemicals Concentration of Deposits on Fracture Surface

In addition, the same corrosion pits are observed on the tenon, blade profile, and root of sound blades of the same stage and turbine as shown in Figure 9. Inside these pits, 2000 ppm Cl is detected. For further investigation, the numbers of corrosion pits are counted on the blades for each stage from the high-pressure section to the low-pressure section in the flow path to compare the corrosion environment level reiteratively. The profile of the measured pit count number in the flow path is shown in Figure 10.
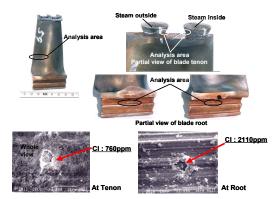

Figure 9 Corrosion Pits on Sound Blade and Corrosive Chemicals Concentration inside of Pits

According to this profile, the frequency of corrosion pits occurrence in the 3 stages (L-2, L-1, L-0: last stage) of the low-pressure section located in the wet zone is high. This is especially the case for the L-1 stage located in the wet/dry transient enrichment zone, which has the highest frequency of corrosion pit occurrence. The profile of the measured concentration of corrosive chemicals that is sampled from the blade surface for each stage is shown in Figure 11. According to this profile and the Cl concentration of the L-1 stage, which is extremely high at around 40000ppm [10] , it is considered that the corrosive chemical enrichment in the wet/dry transient zone and the corrosive environment have a strong relationship with blade corrosion fatigue damage. The threshold of the Cl deposit concentration level for determination which is a cause of general fatigue or corrosion fatigue is around 1000 ppm.
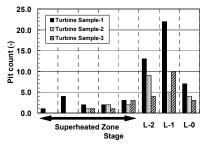
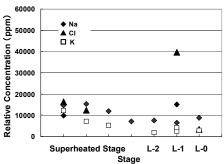*Figure 10 Corrosion Pit No. of Each Stage and Profile*

Figure 11 Corrosive Chemicals Concentration Profile of Deposits

Study of Enrichment Zone and Strength Safety Margin

The separation and deposit, liquid, or solid phases and concentration level of corrosive chemicals on the nozzle and blade profile in each stage are determined by steam temperature and pressure on the turbine designed expansion line and concentration of impurities in steam, which is related to water/steam quality control. The analysis results of Cl concentration in steam expansion and deposit /dissolved condition are shown in Figure 12. This analysis is based on steady chemical equivalent conditions [11] by varying pressure, temperature, and Cl saturated concentration, and focusing on the NaCl supersaturation line in the high concentration zone.
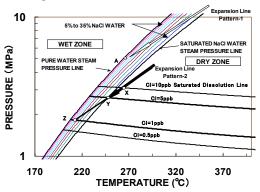

Figure 12 Cl Concentration in Steam Expansion and Deposit/Dissolved Condition

In Figure 12, two different expansion lines are described as arrows "pattern-1" and "pattern-2".

Where Cl concentration reaches 10 ppb for pattern-1, steam expands in the region of high pressure and temperature over the Cl saturation line. Even if the steam condition expands to point-A, the NaCl phase is still gas in

the dry zone and the blade surface is not exposed to high concentrations of corrosive elements in wet conditions.

On the contrary, in the case of 5 ppb, if steam expands in the temperature and pressure of the Cl saturation zone and goes to supersaturation point-Y, water with 30% NaCl, an extremely high concentration, occurs and the blade surface is exposed to a severely corrosive condition. According to these analysis results, even if the Cl concentration is extremely low, such as 1 ppb to 5ppb in steam, a severely corrosive environment can still appear around the blades [12].

However, under actual operating conditions, the blade surface can be washed by steam mist corresponding to moisture in each stage. At the clearance of the tenon and root of the flow stagnation zone, it is difficult to wash and the effect of corrosive chemicals enrichment exceeds the effect of washing. In such conditions, it is considered that the decrease in fatigue endurance limit is accelerated.

On the contrary, steam quality control for maintaining extremely low levels (in the order of several ppb) is practically limited. In order to improve the strength safety margin under actual operations, it is necessary to design the blade structure with a profile and grouping method to decrease both the static and vibration stresses and eliminate the flow stagnation region.

The L-1 stage blade damage is related to the enrichment and concentration level in the wet/dry transient zone, and the vibration stress level. To verify this relationship for damaged and undamaged blades, the relative safety factor of vibration stress based on the allowable limit in the transient zone and measured number of corrosion pit are plotted per each designed stage moisture level as shown in Figure 13. From this result, it is clear that, even if the relative safety factor is sufficient, corrosion fatigue damage occured in the enrichment zone. Furthermore, it is confirmed that the number of corrosion pits is maximum in the enrichment zone, in the same fashion as the profile of the relative safety factor of vibration stress.
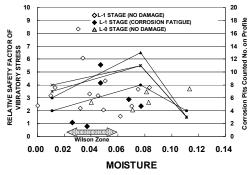

Figure 13 Relation of Wilson Enrichment Zone, Actual Moisture and Fatigue Strength Safety Factor

Study of Corrosion Pits and Crack Propagation

The authors studied the question of whether only a corrosive environment contributes to initial crack generation and crack propagation or the corrosion pit itself contributes by stress concentration as a general fatigue phenomenon. Fatigue tests were conducted in a corrosion

environment by changing the concentration of NaCl to 0.03%, 3% and 22% respectively [13] . The relationship between vibration stress of fatigue test conditions and the observed corrosion pit diameter is plotted on Figure 14. In this figure, the vibration stress range is based on a calculation of the threshold of stress intensity factor [14] , and thus the limit of crack start propagation, as well as the vibration stress measured from detail fracture surface analysis for actual damaged blades, is plotted.
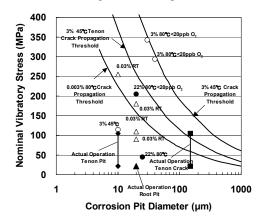

Figure 14 Relation of Corrosion Pit Size and Vibration Stress in Comparison with Crack Propagation Limit Line

According to these results, if a corrosion pit of over 100 micrometers diameter has a vibration stress of less than 100MPa, there is a possibility of crack propagation. Under a severe corrosive condition of 22%NaCl concentration, together with a small amount of oxygen, even if a low vibration stress acts on the blade, small corrosion pits of 20 micrometers are observed and finally fatigue failure occurred. Based on the fact that the blade actually failed under low vibration stress and several corrosion pits were observed, it can be concluded that a corrosive environment eavily contributes to initial crack generation, but crack propagation and corrosion pitting themselves don't seem to contribute to stress concentration.

Conventional blades have a tenon, and after tenon caulking from plastic forming, micro wrinkle occurs. It is suspected that this micro wrinkle contributes to crack propagation as a stress concentration or stress raiser in certain conditions. In Figure 15, the stress intensity factor calculated from the actual observed wrinkle depth and acting vibration stress is compared to the threshold of stress intensity factor. This figure tells us that if a large excitation force over 10 times that calculated acts on a blade, there is a possibility of crack propagation from micro wrinkles in tenon caulking.
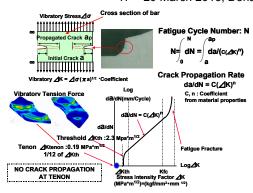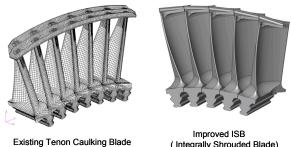

Figure 15 Tenon Caulking Stress Raiser and Crack Propagation Limit

Improved Blade for Corrosion Fatigue Prevention

From the above, it was concluded that the strength safety margin of conventional tenon caulking finite grouped blades has to be improved for an application of L-1 stage under the wet/dry transient zone for high speed and high loading turbine (such as synthesis gas compressor drivers), when considering the difficulty or limitation for water/steam quality control.

Figure 16 Improved ISB for Corrosion Fatigue Strength

Having reached this conclusion, as shown in Figure 16, ISB [15] was developed by applying the blade profile and shroud in one piece without a tenon . These blades are thus infinitely grouped with a twist back torque mechanism as shown in Figure 17 in order to eliminate lowest frequency tangential load in phase mode and increase natural frequency. For this improved ISB, a stress analysis has been completed and sufficient improvement of safety factor confirmed [16] . Furthermore, this ISB has been applied on actual turbines and successfully operated.
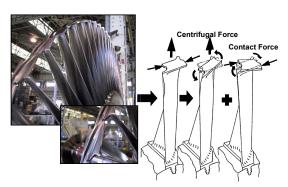

Figure 17 Mechanism of ISB Twist Back Infinite Coupled [16]

Surface Treatment Methods and Features for Prevention of Flow Path Damage

The authors have introduced blade structure improvements in order to increase the safety margin for corrosion fatigue. A key factor related to performance deterioration and operation restriction needing emphasis is fouling on nozzle and blade profiles. It is necessary to think of some improvement for the prevention of such fouling. Accordingly. the authors have studied surface treatment methods applied to actual blades to improve anti-corrosion and anti-fouling.

Applicable surface treatments for rotating machines to prevent classified damage phases are shown in Table 1. Several surface treatment methods corresponding to operation environment have been applied for prevention of erosion damage by solid particles and water droplets, fouling on the flow path, and corrosion fatigue. Recently developed and improved methods are boronizing, ion plating, plasma transfer arc welding, and radical notarization plus Nickel Phosphate multilayer hybrid coating. These methods are introduced in this paper.

Table 1   Damage Phase and Surface Treatment

PHENOMENA	SOLID PARTICLE EROSION(SPE)	DRAIN ATTACK EROSION(DAE)	DEPOSITS FOULING	CORROSION FATIGUE
MECHANISM	PLASTIC DEFORMATION DAMAGE	DUCTILE FATIGUE DAMAGE	PHASE CHANGE & SURFACE ENERGY	CHEMICAL ENRICHMENT & POTENTIAL VOLTAGE
TEMPERATURE	HIGH	LOW	HIGH TO LOW	LOW WET ZONE
APPLICABLE COATING ●: LOW BONDING STRENGTH SHORT LIFE ◆:NEW TECHNOLOGY HIGH BONDING LONG LIFE	● PLASMA SPRAY ◆ BORONIZING ◆ RADICAL NITRIZATION&CrN	● STELLITE PLATE BRAZING ● PLASMA SPRAY ◆ ION PLATING ◆ PTA	● INORGANIC PAINTING & INORGANIC SEALANT ● FLUORINE COATING ◆ NI-P HYBRID PLATING	● INORGANIC /ORGANINC PAINTING & PTFE SEALANT ◆ RADICAL NITRIZATION Ni-P MULTI LAYER HIBRID COATING
APPLICATION	NOZZLES DIAPHRAGM	BLADES NOZZLES DIAPHRAGM	BLADES NOZZLES	BLADES NOZZLES DIAPHRAGM

Furthermore, multilayer hybrid spray coating is applied for compressor impeller assemblies to prevent or relax fouling of internals as shown in Table 2. However, the bonding strength for this type of coating is generally low and it is difficult to maintain the initial coating function during long-term operation.

Table 2   Typical Conventional Coating Specification

Applicable Component	Nozzles and Blades of High pressure Stages or Low Pressure Stages DISADVANTAGE : SHORT LIFE DUE TO LOW BONDING STRENGTH			
Purpose of Use	Prevention of Corrosive Fatigue due to Corrosive Chemicals Invasion Relaxation of Fouling			
Coating Specification		Type	Temperature	Coating Procedure	Coating Layer Formation
		A	High 566deg.C ~ 260deg.C	Inorganic Painting ↓ Inorganic Sealant Treatment	Thickness 50μm Chromate & Phosphate Chemical Inert Sealant, Galvanic Sacrificial Coating, Blasting Treatment, Base Metal
		B	Low less than 260deg.C	Inorganic Painting ↓ Organic Painting ↓ PTFE Sealant treatment	Thickness 150μm PTFE Base Top Coating, Polymeric Inhibitive Coating, Galvanic Sacrificial Coating, Blasting Treatment, Base Metal

Requirement of Features for Blade Surface Treatment and Concept of Developed Coating

In order to prevent both steam turbine performance deterioration and blade strength margin decrease during long-term operation, a new surface treatment is necessary to meet requirements of solid particle erosion prevention, anti-fouling, anti-corrosion, and drain erosion protection corresponding to steam temperature and pressure for each stage as shown in Figure 18. In this study, the requirements are defined as shown below for the low pressure section of steam temperature which is lower than 350 deg.C, as follows: 1) Prevention or relaxation of fouling on nozzle and blade profiles, 2) Improvement of washing efficiency during online washing, 3) Prevention of decrease in corrosion fatigue strength, 4) Anti-drain erosion performance in the same way as base materials
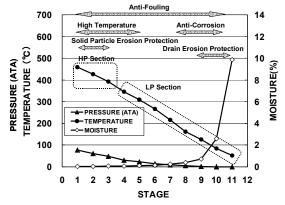

Figure 18 Turbine Internal Condition and Coating Required Function

One of the main factors affecting fouling on the blade profile surface is the material surface energy. As shown in Figure 19, PTFE has a lower surface energy than other types of ceramics and this is therefore suitable for prevention of fouling. However, PTFE's own strength is low and it is necessary to improve coating performance with a hybrid for actual application.
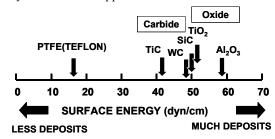

Figure 19 Several Types of Ceramics and Surface Energy Level

In order to realize a new suitable and multi-function coating considering the bonding strength between the anti-fouling coating layer and base metal, anti-erosion (prevention of layer separation) and anti-corrosion, a new coating has been developed. This coating concept is shown in Figure 20.

Compression stress is produced in the surface of the base

metal with a radial nitriding surface treatment. Furthermore, a Galvanic Ni Coating layer is formed to improve bonding condition and coherency.   A Ni-P PTFE Hybrid coating is formed to realize the combination of reduced surface energy for improved anti-fouling and bonding force. Finally, a top PTFE dispersion coating is formed to further reduce surface energy more.
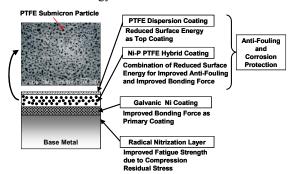

Figure 20 Basic Concept of Developed Coating

Systematic Evaluation Test and Results for Developed Coating

A systematic evaluation test was carried out to understand the characteristics of the newly designed hybrid coating layer (based on new concepts including top coating) and compared with conventional coating. As shown in Table 3, coating test pieces were prepared for each evaluation parameter such as surface roughness, PTFE dispersion ratio, and layer thickness. Figure 21 shows an overview of the coating test pieces corresponding to Table 3. Coating evaluation test items and target requirements are summarized in Table 4.

The procedures to simulate actual operation in terms of fouling, washing and drain erosion were developed and applied.

Table 3 Coating Test Pieces and Evaluation Parameter

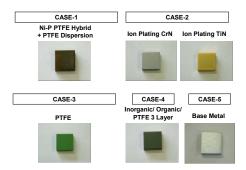| Case No.	Sample Base Coating Type	Coating Parameter for Performance Evaluation
1	Ni-P PTFE Hybrid Coating	● PTFE Dispersion Ratio on Surface
2	PVD Physical Vapor Deposition	● Surface Roughness ● Layer Materials(TiN,CrN)and Thickness ● Deposition Procedure (Ion Plating,etc)
3	Fluorine Simple Coating	● Fluorine Materials (PTFE, etc) ● Layer Thickness
4	Inorganic/ Organic/ PTFE Three Layer Paint Coating	● Layer Thickness
5	Base Metal (SUS410J1)	● Surface Roughness

Figure 21 Overview of Coating Test Pieces

Table4 Coating Evaluation Test Items

TEST NO.	EVALUATION POINTS	TEST PROCEDURE	TARGET REQUIREMENT
1	Fouling Resistance	SiO_2 nanometer powder jet injection under hot wet condition	1/2 Deposit of Base Metal
2	Washing Efficiency	Steam Jet Washing	1/2 Washing Duration of Base Metal
3	Corrosion Fatigue Strength	3% NaCl Solution Rotating Bending Fatigue Test	Better than Base Metal
4	Erosion Resistance	High Frequency Cavitations Erosion Test	Same as Base Metal
5	Coating on Actual Blade Profile	Masking Immersion and Spray	Layer Thickness Profile

Anti-Fouling Characteristics Evaluation Test

An anti-fouling test set up for simulating fouling conditions so that deposits will form on the material surface has been designed and manufactured according to the theory of cohesion and adhesion engineering of micro fine particles.   For the basic fouling test procedure, fine particle material, diameter and particle collision velocity were adjusted the same as actual conditions and the amount of particle concentration was increased for acceleration of fouling conditions.   Figure 22 shows the anti-fouling test set up and Table 5 shows the test conditions.   The rotating drum is heated up to 500 deg.C and Silica fine particles are sprayed over the test pieces at a velocity of 300 m/sec. The ease of fouling is evaluated relatively by measuring the weight increase of deposit on the test piece surface during over a 200-hour test period.   Figure 23 shows the surface deposit condition during this 200 hours of spraying each test piece.   An anti-fouling index (difficulty to deposit) is defined as the ratio of deposit weight based on SUS 410J1 base metal. The relationship between this anti-fouling index and surface roughness for each test piece is shown in Figure 24.
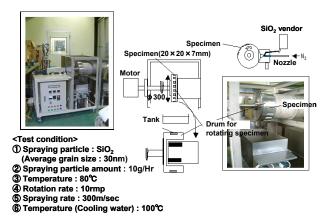
<Test condition>
① Spraying particle : SiO₂
   (Average grain size : 30nm)
② Spraying particle amount : 10g/Hr
③ Temperature : 80℃
④ Rotation rate : 10rmp
⑤ Spraying rate : 300m/sec
⑥ Temperature (Cooling water) : 100℃

Figure 22 Anti-Fouling Test Set-Up

Table5 Micro Powder Deposit Test Condition

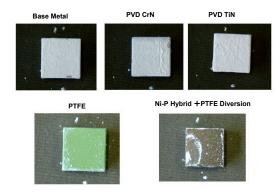| Test Item	Condition
1.Spray Micro Powder	Silica Powder Average Diameter 10nm
2.Spray Flow Rate	10g/Hr
3.Powder Velocity	300m/s
4.Surface Temperature	80℃
5.Environment	Water Supply
6.Rotating Speed	10rpm

Figure 23 Surface Deposit Condition after 200Hrs Spray
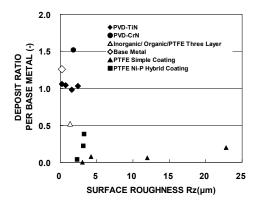

Figure 24 Surface Roughness and Deposits Ratio

According to this result, PTFE Ni-P hybrid coating has almost the same anti-fouling characteristics as PTFE coating. The change in the anti-fouling index for PTFE Ni-P hybrid coating, when changing the occupation ratio

for PTFE dispersion in the top coating is shown in Figure 25. With a 20% occupation ratio of PTFE dispersion and practical surface roughness, the anti-fouling index can be decreased to 1/5 of the base material. Furthermore, this coating performance is twice as effective as the conventional spray paint coating usually applied for a compressor.

According to this result, PTFE Ni-P hybrid coating has almost the same anti-fouling characteristics as PTFE coating. The change in the anti-fouling index for PTFE Ni-P hybrid coating, when changing the occupation ratio for PTFE dispersion in the top coating is shown in Figure 25. With a 20% occupation ratio of PTFE dispersion and practical surface roughness, the anti-fouling index can be decreased to 1/5 of the base material. Furthermore, this coating performance is twice as effective as the conventional spray paint coating usually applied for a compressor.
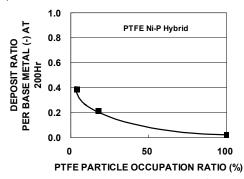

Figure 25 PTFE Occupation Ratio and Deposit Ratio

Washing Efficiency Evaluation Test

If an anti-fouling coating is formed on the nozzle and blade profile surface, chemical contaminants tend to deposit on the profile surface during long-term operation. In order to resolve this problem, a new technique of on-line washing can be applied for a steam turbine with water injection into the valve chest and steam change from the dry to wet zone as the previously described [17]. In this study, washing efficiency is evaluated with a selected anti-fouling coating.
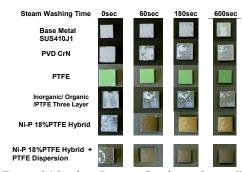

Figure 26 Surface Deposit Condition during Washing

An evaluation procedure for the simulation of actual washing has been developed by applying steam injection to test pieces with deposits after a 200-hour fouling simulation test period. The washing efficiency is evaluated quantitatively by the weight of removed silica deposit and qualitatively by an overview of the washed surface. Figure 26 shows an overview of surface deposit conditions during

washing and Figure 27 shows SiO_2 deposit removal mass during washing. The SiO_2 deposit removal time is listed in Table 6.
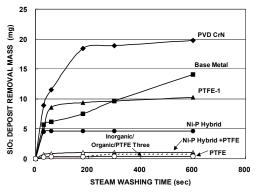

Figure 27 SiO₂ Deposit Removal Mass during Washing

From these results it can be concluded that the selected PTFE Ni-P hybrid coating has the same washing efficiency as a PTFE single coating. By comparison of the deposit weight ratio and complete removed washing time ratio among the various test piece coating types, it is thought that the relative washing speed of the PTFE Ni-P hybrid coating is larger than other types of coating and base metals.

Table 6 SiO₂ Deposit Removal Time

Test Sample	SiO₂ Complete Removal Time (sec)
Ni-P PTFE Hybrid + 18% PTFE Dispersion	180
Ni-P 18% PTFE Hybrid	180
PTFE	30
PVD CrN Low Surface Roughness	> 600
Inorganic/Organic/PTFE Three Layers	> 600
Base Metal SUS410J1	> 600

Anti-Erosion Evaluation Test

An anti-erosion evaluation test was conducted in accordance with ASTM G32-77 [18] using the cavitations erosion accelerated test set-up shown in Figure 28. The results of this test are shown in Figure 29. The wear mass reduction of the Ni-P PTFE hybrid coating is much smaller than that of the PTFE single coating and larger than that of the base metal at the beginning of the test. However this wear mass reduction is expected to saturate to a level smaller than that of the base metal at the end of the test.
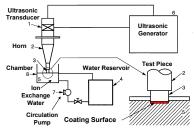

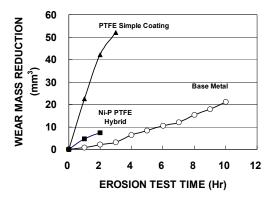*Figure 28 Cavitations Erosion Accelerated Test Set-Up*

Figure 29 Accelerated Erosion Test Results

Corrosion Fatigue Test

A rotary bending fatigue test was conducted for the PTFE single coating and the radical nitriding Ni-P hybrid coating under normal atmospheric conditions and very severe corrosive conditions, with 3% NaCl distilled water. The test results are shown in Figure 30 and Figure 31 respectively. Under normal atmospheric conditions, the fatigue endurance limit for both of the PTFE single coating and the radical nitriding Ni-P hybrid coating is 400MPa at 1×10^7 cycles, almost the same as base metal SUS410J1 applied for blades and nozzles.
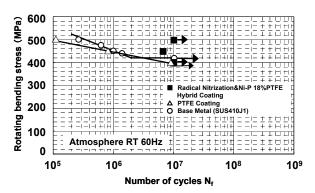

Figure 30 Fatigue Test Result at Atmosphere

However, with 3% NaCl distilled water, the fatigue failure rotating bending stress decreased to 200 MPa at 1×10^8 cycles for the PTFE single coating, 100 MPa at 4×10^7 cycles for the base metal, and 150 MPa at 1×10^8 cycles for the radical nitriding Ni-P hybrid coating. This is twice the corrosion fatigue resistance than the base metal. It is thought that the reason why the corrosion fatigue resistance is improved with both coatings is because the coating layer is very fine with fewer defects (such as pin holes), and that they contribute to the effect of environment interception. In addition, in the LCF region of high stress, the corrosion fatigue resistance of these coating has improved, which means that the layer itself has a high level of toughness and high bonding strength with the base metal.
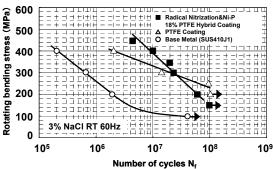
Figure 31 Corrosion Fatigue Test Result

Coating Application of Actual Blades and Additional Improvement for Prevention of Steam Turbine Efficiency Deterioration

Following the results of this study and the evaluation tests as explained above, the PTFE Ni-P hybrid coating was applied to the actual blade as shown in Figure 32. Additional improvement measures for prevention of steam turbine efficiency deterioration were applied to an actual steam turbine as shown in Figure 33 and listed below. ISB [19] was applied for all stages (impulse and reaction types) to increase overall efficiency and prevention of corrosion fatigue in the dry/wet transient zone. For inlet 1st stage nozzles, boronizing coating was applied to prevent solid particle erosion and last-1 and last stage blade surfaces were treated with TiN ion plating and PTA (plasma transfer arc welding) respectively to prevent drain erosion. In addition, wide pitch nozzles were applied for all stages to increase stage efficiency and to minimize after stage pressure due to fouling.

Ni-P 18%PTFE Hybrid

Figure 32 Coated Actual Blade

Figure 33 Improvement of Blade Integrity, Coating Application of Actual Blades and Additional Improvement for Anti-efficiency deterioration

In Figure 34, the difference in after stage pressure increase due to deposits on the nozzle profile is explained by comparing a fine pitch nozzle and wide pitch nozzle. If deposit thickness increase rate (mm/year) is the same, the nozzle area reduction rate of wide pitch nozzles can be decreased by half because of the smaller number of nozzles or smaller profile surface area than the fine pitch nozzle. After-stage pressure increase is proportional to steam flow and this turbine can have more margin for operating time reaching the pressure limitation under fouling conditions, whilst maintaining the required power and extending operation time.

Furthermore, if online washing is executed periodically, the operating time can be extended more by performance recovery.
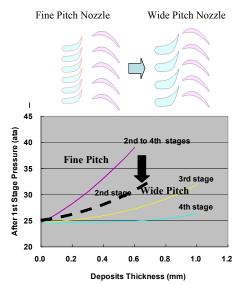

Figure-34 Wide Pitch Nozzle to Minimize Pressure Increase due to Fouling

Figure 35 explains the advantage of each improvement and their combination. In this case study, the power recovery ratio after online washing is assumed to be 80% and the power decrease rate due to after-stage pressure increase caused by fouling is half of a fine pitch nozzle when using a wide pitch nozzle application.

This new online wash technology has been applied for over 20 turbines and typical successful results on site are shown in Figure 35 [20] [21]. In this case, an anti-fouling coating such as an Ni-P PTFE hybrid multi layer coating is not applied. However, it has been confirmed that the turbine performance recovers after online washing to the original clean condition. If this newly developed coating and other improvements, including online washing and wide pitch nozzles as explained above are applied systematically, the turbine integrity and performance can be maintained to the same as the original during long-term operation over 8 years [22] [23] [24] [25] [26].
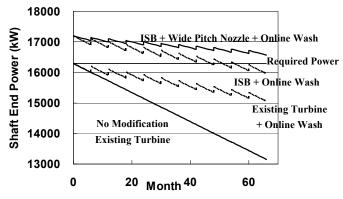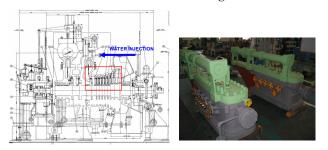
Figure 35 Advantage for combination of Wide Pitch, All ISB and On-line Washing
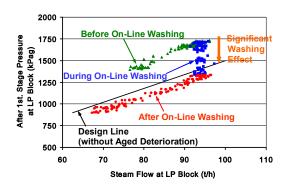

On-Line Washing Results

Figure 36 Successful On-line Washing at Site

Detail Investigation of Steam Turbine Internal Phenomena during On-line Wash

The steam turbine online wash procedure had already been established and applied in more than 30 actual turbine applications. The water is directly injected inside of the turbine valve chest and typically it is not necessary to reduce the power and speed. During several-hour-short-duration online washing, the LP section condition becomes wet and washable chemicals are washed out as indicated by a high spike of conductivity. After several hours of washing, the extraction pressure decreases to a level much lower than the allowable pressure limit and the turbine performance increases as shown in Figure 36. Before and after washing, the operating conditions, including power based on measured torque are compared and typical results are shown. A large increase in the power recovery ratio is confirmed.

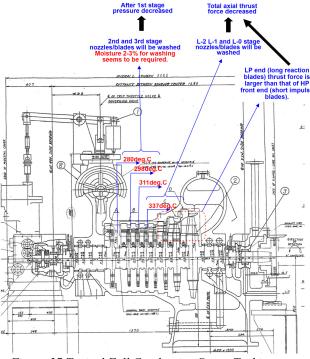It is important to understand the turbine internal condition during on line wash for increasing wash effectiveness and to optimize on line wash procedure.

Figure 37 Typical Full Condensing Steam Turbine for On-line Washing

As a typical case of on line wash for investigation of thermodynamic condition in flow path, the full condensing steam turbine shown in Figure 37 is selected.

The expansion curve during of this steam turbine during on line wash is shown in Figure 38 on i-s chart, according to this curve, the moisture for each stage can be estimated.
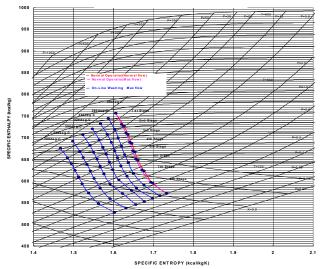

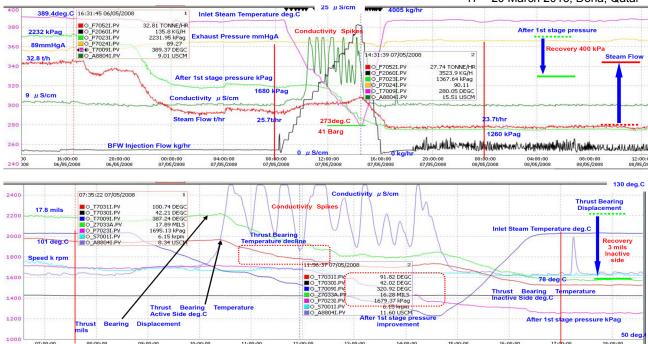*Figure 38 Expansion Curve during On line Wash*

Figure 39 Operation Trend Data Summarized during Online Wash

Top graph of Figure 39 shows the change of operation conditions in decreasing inlet temperature by injecting boiler feed water. In this case, inlet steam flow is reduced from normal condition to have a safety margin and minimalize any risk and normally 10% steam flow reduction is recommended. During deceasing inlet steam temperature from 389 deg.C to 273 deg.C, there are a number of distinct conductivity spikes and it is seemed that the position of the moisture point inside the turbine moves across more than one wheel and diaphragm or it concentrates more locally around one row position. also is showing the regain that we have made in the wheel chamber pressure. After returning to full load condition, the after 1st stage pressure has recovered approximately 400KPA after completion of wash.

Bottom of this graph shows the effect of removing fouling has on thrust bearing temperature and axial position of rotor. It is observed that the majority of temperature decline in active thrust bearing is occurring earlier than when wheel chamber pressure is starting to improve.

The axial position of the rotor has also moved 3mils back after cleaning of rotor and the thrust bearing pad metal temperature goes down from 101 deg.C to 78 degC.

CONCLUSIONS

For mechanical drive steam turbines, the investigation results of corrosion fatigue phenomena in the transient zone have been introduced including basic phenomena on the expansion line and actual design and damage experience. These results were analyzed from the standpoint of stress intensity during the start of cracking. In order to resolve these problems, preventive coating and blade design method against fouling and corrosive environments have been developed. Detailed evaluation

and on-line washing results on site were introduced.

Following the results of this study and the evaluation tests, a PTFE Ni-P hybrid coating has been applied to the actual blades for prevention of steam turbine efficiency deterioration. Other improvements including online wash and wide pitch nozzles have been applied systematically. As a result, the turbine integrity and performance can be maintained the same as the original machine throughout long-term operation.

In addition, the detail investigation of steam turbine internal condition during on line wash were conducted in terms of thermodynamics, necessary moisture, the thrust load change and vibration related to washing condition based on typical on line wash trend data.

Appendix

Strength Analysis and Evaluation in comparison with Operation Experience

The results of static stress and dynamic stress analysis for the actual failed blade shown in Figure 3 are shown in Figure 40 to Figure 42. The tenon has the maximum peak static stress at its outside, which is a different location from the actual crack initiation point. However, the location of crack initiation has a minimum safety margin and this margin has to be evaluated according to both static and dynamic stress on a Goodman diagram. To analyze the dynamic vibration stress, a 3D solid model is made for one group of blades, including the rotor disk to take account of the couple modes of the blades and disk as one vibration system. The natural frequency for each mode is calculated and plotted on a Campbell diagram as shown in Figure 41.
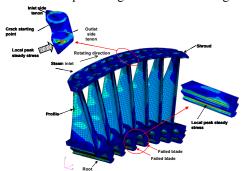

Figure 40 Static Stress Analysis Result

The resonance points are identified in the operation speed range and analyzed to determine the vibration response of the excitation force at resonance point [7]. In case of finitely grouped blades, the vibration stress becomes largest at resonance with lowest frequency harmonic tangential in-phase mode. The excitation force is given on the blade profile calculated from pressure distribution of a steady CFD analysis and stimulus of fluctuation level per steady level and harmonic number. The vibration response is calculated in relation to system damping. The vibration stress profile (contour) is shown in Figure 42 and the maximum peak vibration stress is observed on the inside of the tenon and stress concentration point of corner radius, which is the same as the actual crack initiation point.
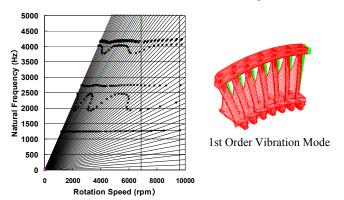

1st Order Vibration Mode

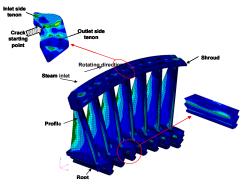*Figure 41 Campbell Diagram and Operation Range*

Figure 42 Vibration Stress Analysis Result for 1st Mode

The same standard blades have been applied to over 80 turbines, which have all been in long-term operation. Among them, three turbines have the same blade damage. The static stress and vibration stress for each turbine is plotted on the Goodman diagram shown in Figure 43, comparing the allowable fatigue limit corresponding to a wet and dry transient Wilson zone [8]. Considering the fact that vibration stress is very small and lower than this limit, and this blade damage happened after long-term operation, it is expected that the blade damage is caused by a corrosive environment related to unsuitable water and steam quality control.
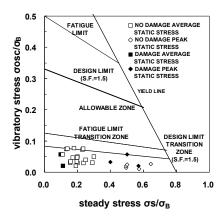

Figure 43 Design Experience on Goodman Diagram

Chemical Materials Deposition on Flow Path and Performance Deterioration

During steam turbine continuous long-term operation, steam contaminants, such as silicate and sodium, deposit on the internals as solids. This occurs under certain operating conditions related to steam pressure and temperature for each of the stages. These contaminants foul the surfaces of nozzles and blades and gradually build up during steam turbine operation. Figure 44 shows the fouling condition after 7 years of continuous operation.

Figure 44 Deposit Condition of LP Section

The composition and characteristics of the fouling materials are different along the steam path from the high-pressure stages to the low-pressure side. Under these fouling conditions, the pressure profiles across the nozzles, blades, and throat areas increase. These profiles in turn result in the deterioration of turbine performance, and it will continue to do so over time if left unattended. The authors have calculated the relationship between after stage pressure increase and efficiency change (loss) due to the fouling thickness within the high and low pressure sections. When fouling happens and the nozzle profile has deposits, the nozzle area is reduced, and the nozzle exit speed and velocity ratio per stage change. This velocity ratio is directly related to stage efficiency and overall efficiency of the HP and LP section. The typical calculation result for the HP section is shown in Figure 45. According to this thermodynamic calculation and analysis, the HP section efficiency is more sensitive than that of the LP section where each stage profile has the same fouling thickness.

Overall efficiency change and after stage pressure change depend on what stage has deposits and its fouling thickness.
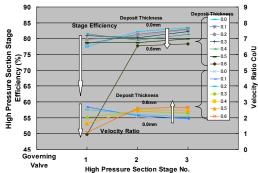

Figure 45 Blade Design, Efficiency affected by Fouling in Each Stage

Moisture Profile during Reduction of Inlet Temperature
Figure 46 shows the calculated moisture change of internals when inlet temperature deceases from normal to the lowest during washing. At the normal inlet steam temperature, only 6th to 8th stage locate on wet zone and maximum moisture is about 9%. In case of the lowest inlet temperature 260deg.C, all stages are located lower than saturated line and the maximum moisture of last stage becomes 17%. The on line wash condition have to be
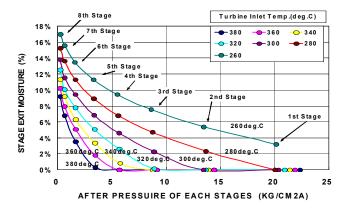
optimized in considering what stage has the fouling and what is the allowable limit of high moisture in terms of erosion damage and countermeasures for protection   such as ceramics coating, PTA power welding and stainless steel diaphragms .

Figure 46 Moisture Profile during Reduction of Inlet Temperature

Relationship between Inlet Temperature, Moisture at Each Stage and Conductivity Spikes
In Figure 47, these relations are shown including time delay of axial thrust displacement decrease (thrust force decrease) and after 1st stage pressure recovery.
In case of Inlet temperature going down to about 340 deg.C, L-2 L-1 and L-0 stage nozzles/blades are washed, in addition, LP end (long reaction blades) thrust force is larger than that of HP front end (short impulse blades). Accordingly, total axial thrust force decreases. After 1st stage pressure is dominantly affected by the 2nd and 3rd stage nozzles/blades area reduction.
In case of Inlet temperature going down to the range of about 310 to 280 deg.C, the 2nd and 3rd stage nozzles/blades are washed and in this inlet temperature range, after 1st stage pressure decreased. Minimum moisture for washing is expected 2 to 3% and when moisture of each stage increases cross this threshold, conductivity spike occurred.

Thrust Force Reduction and Axial Displacement after Online Wash
Figure 48 shows change of axial displacement and pad metal temperature related to thrust bearing performance.
We expect thrust force deceases from 20-25 kgf/cm^2 of bearing pressure (intensity) to 10 kgf/cm^2 of normal as designed. Almost change of axial displacement (about 100 micron meter) is elastic deflection of leveling plates and oil film thickness increases by 30 micron meter as your pointing out.

Figure 47 Relationship between Inlet Temperature, Moisture at Each Stage and Conductivity Spikes

Levering plates for Equalizing have elastic deflection 0.12mm, Levering plate elastic deflection is larger than oil film thickness change

*Figur*e 48 Thrust Force Reduction and Axial Displacement after Online Wash

Vibration phase change and correspondence to conductivity spikes during online washing

Rotor response is summarized in Figure 49, 1 time vibration phase increase / decrease has the relationship with conductivity spikes (up/down). In case of 1 time vibration, amplitude does not change, only phase changes.

On the contrary, in case of 2 time vibration, amplitude changes and phase does not change. It is expected that excitation force in rotating in drain or mist and unbalance caused by partial washing during washing start affect rotor response. The detail investigation is necessary.
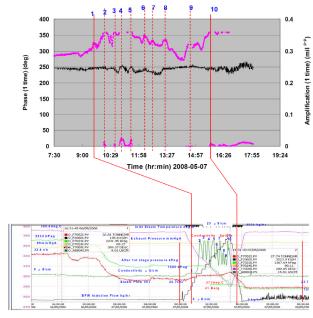

Figure 49 Vibration phase change and correspondence to conductivity spikes during online washing

Acknowledgement

References

[1] Saga.M, Hata. S. et al., Repair Technologies of Mechanical Drive Steam Turbines for Catastrophic Damage, Proceedings of the 34th Turbomachinery Symposium (2005), pp. 15-23.

[2] The ASME Handbook on Water Technology for Thermal Power Systems p12

[3] J Jonas Otakar, Understanding Steam Turbine Corrosion 84 (1984) pp55 2 -55 28

[4] Ebara Ryuichiro, et al., Corrosion Fatigue Behavior of 13Cr Stainless Steel for Turbine Moving Blade, Mitsubishi Heavy Industry Technical Bulletin Vol.15 No.3 May 1978, pp1-10

[5] Naumann Hekmut G., Steam Turbine Blade Design Options: How to Specify or Upgrade, Proceedings of 11th Turbomachinery Symposium, pp29-49

[6] Kihara Hiroshi, Fractography

[7] Wagner L.F, Griffin J.H, Forced Harmonic Response of Grouped Blade Systems: Part I -Discrete Theory, Transaction of the ASME, Vol.118, January 1996, pp130-136

[8] Ebara Ryuichiro, et al., Corrosion Fatigue Strength of 13 Cr Stainless Steel for Steam Turbine Blades, Mitsubishi Heavy
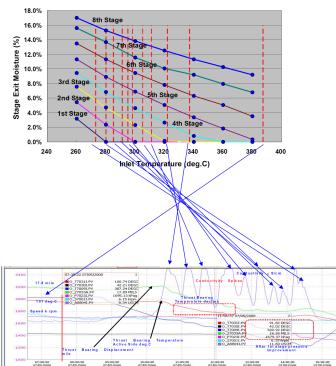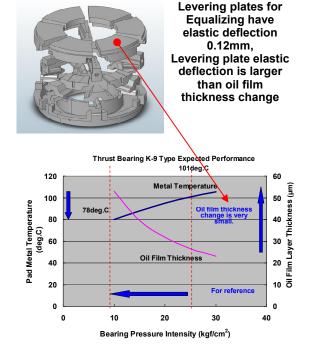
Industry Technical Bulletin Vol.19 No.5 September 1982, pp537-543

[9] Ebara Ryuichiro、Japan Steel Society , Nishiyama Memorial Technical Session, Environment Crack of Steel, October, 1982

[10] Ebara Ryuichiro, et al., Corrosion-Fatigue Behavior of 13Cr Stainless Steel in Sodium-Chloride Aqueous Solution and Steam Environment, American Society for Testing and Materials, Corrosion-Fatigue Technology, pp155-168

[11] Steltz W.G, et al. Verification of Concentrated Impurities in Low Pressure Steam Turbines, Transactions of the ASME, Vol.105, January 1983, pp192-198

[12] Bischoff James L, et al. Liquid-Vapor Relations for the System NaCl-H2O: Summary of the P-T-x Surface from 300℃ to 500℃, American Journal of Science, Vol.289, 1989, pp217-248

[13] Allmon.W.E. et al., Deposition of Salts from Steam, International Water Conference (1983), pp127-138

[14] Maday M.F. et al., Stress Corrosion Cracking Behavior of Two Ni-Cr-Mo-V Steels in Caustic Solutions and Pure Oxygenated Water, Corrosion Vol.45, No.4, pp273-281

[15] Ebara Ryuichiro .et al., Corrosion Fatigue Process of 12 Cr-Stainless Steel, ISIJ Inter-national, Vol.30 (1990), No.7, pp535-539

[16] Katayama Kazuso, et al., High-Speed and Large Capacity Compressor-Driving Turbines for Chemical Plants, Mitsubishi Heavy Industry Technical Bulletin Vol.14 No.5 September 1977, pp1- 9

[17] Bhat. G.I., Hata. S. et al., New Technique for Online Washing of Large Mechanical–Drive Condensing Steam Turbines, Proceedings of the 33rd Turbomachinery Symposium (2004), pp.57-65.

[18] Hata. S. et al., Recent Technologies for the Reliability and Performance of Mechanical-Drive Steam Turbines in Ethylene Plants, Proceedings of the 34th Turbomachinery Symposium (2005), pp.15-23.

[19] Hata, S., Sasaki, T., Ikeno, K., New Technologies of Synthesis Gas Compressor Drive Steam Turbines for Increasing Efficiency and Reliability, Proceedings of the 31st Turbomachinery Symposium, Houston, (2002), pp.75-83.

[20] Hata, S., New Technique for Online Washing of Large Mechanical–Drive Condensing Steam Turbines, Proceedings of 2007 AIChE Spring National Meeting Ethylene Producer Conference, Houston, (2007).

[21] Hata, S., Case Study: Assessing a New Technique for Online Washing of Large Mechanical–Drive Condensing Steam Turbines, Proceedings of ROTATE 2007, UAE Abu Dhabi, (2007)

[22] S. Hata, T. Hirano, N., T. Wakai, H. Tsukamoto, New On Line Washing Technique for Prevention of Performance Deterioration due to Fouling on Steam Turbine Blades (1st Report: Fouling Phenomena, Conventional Washing Technique and Disadvantages), Transaction of JSME Div. B, Vol.72, No.723, November 2007, pp2589-2595.

[23] S. Hata, T. Hirano, N., T. Wakai, H. Tsukamoto, New On Line Washing Technique for Prevention of Performance Deterioration due to Fouling on Steam Turbine Blades, (2nd Report: Basic Experiment and Analysis for Actual Operation of Washing System), Transaction of JSME Div. B, Vol.72, No.724, December 2007, pp2970-2979.

[24] S. Hata, T. Miyawaki, N. Nagai, T. Yamashiata, H. Tsukamoto, Study on Corrosion Fatigue Phenomena of Low Pressure Blades and Integrity Improvement for Mechanical Drive Steam Turbines (1st Report: Relation of Corrosive Chemicals Enrichment Zone and Corrosion Fatigue), Turbomachinery, Vol.35, No.2, February 2007, pp8-16.

[25] S. Hata, T. Yasui, K. Yamada, H. Tsukamoto, Study on Corrosion Fatigue Phenomena of Low Pressure Blades and Integrity Improvement for Mechanical Drive Steam Turbines (2nd Report: Operation Life Extension by Blade Surface Treatment and Coating), Turbomachinery, Vol.35, No.3, March 2007, pp50-59.

[26] S. Hata, Blades Improvement for Mechanical Drive Steam Turbines, Coating Technologies applied for Nozzle and Blade of Mechanical Drive Steam Turbine, Turbomachinery, Vol.29, No.5, May 2001, pp40-47.